Catalytic Wheel as a Brownian Motor

V. M. Rozenbaum,*,†,‡ D.-Y. Yang,† S. H. Lin,† and T. Y. Tsong§

Institute of Atomic and Molecular Sciences, Academia Sinica, P.O. Box 23-166 Taipei, Taiwan, Institute of Surface Chemistry, National Academy of Sciences of Ukraine, Generala Naumova str. 17, Kiev, 03164 Ukraine, Institute of Physics, Academia Sinica, Taipei, Taiwan, and College of Biological Sciences, University of Minnesota, St. Paul, Minnesota 55108

Received: April 25, 2004; In Final Form: July 16, 2004

A system is considered in which transitions between two states occur through two reaction channels. Because of coupling with an external process which consists of cyclic switching between two regimes (each characterized by a certain fixed set of rate constants), the net circulation flux arises in the system even in the absence of an external generalized force. Such a mechanism underlying a catalytic wheel of many biological processes is considered as a Brownian motor. The basic operational motor characteristics are calculated for the regular and random inter-regime switching, being better in the former case and reaching the optimum at equal relaxation-to-lifetime ratios for the two regimes. The general Brownian motor formalism is exemplified by two particular realizations, the electroconformational-coupling model and the flashing-potential model. The former concerns enzymatically catalyzed ligand pumping through a membrane, and the latter describes particle motion under two sets of potential wells and barriers. Because of a unified thread between the two models, their parameters are interrelated, and all of the relevant conclusions are valid for either of them. In the tight coupling limit, the optimal conditions are analyzed, and they imply that a catalytic wheel operated by the Brownian motor works with the maximum output energy (useful work) or with the maximum efficiency tending to unity under certain conditions.

I. Introduction

The conversion of various forms of energy into directed motion on the nanoscale has attracted considerable interest in recent years.[1−3] This problem arises in various contexts.[4] The main motivation comes from molecular biology: the energy provided by a chemical reaction, the hydrolysis of adenosine triphosphate, is used by molecular motors to move along a biopolymer or by molecular pumps to pump ligands and ions across a membrane. Insight into the operational mechanisms of protein motors and molecular pumps has been an objective of much research.[1−4] Another instance is concerned with nanoscale machinery, where there exists the problem of the fed energy transformation into directed motion of the microscopic engine.[5,6] One more example comes from separation science, where external noise can play a constructive role forcing particles of different size to move in opposite directions.[2,7]

Mechanochemical coupling[8] of two processes giving rise to directed motion is describable in terms of the Fokker−Planck approach if detailed evidence on the chemical process is available and a continuous "reaction coordinate" in the phase space[9−11] can be introduced. However, the approach based on chemical kinetics often proves preferable in consideration of complicated chemical processes because it enables an easier analytical treatment.[12,13] In terms of chemical kinetics, an external cyclic process dictates the rate constant values relevant to the directed-motion generation. Clearly, the former process appears to be a kind of a catalyst, inducing the process of directed-motion generation in the system concerned. The coupling of the two processes can be exemplified by the model of electroconformational coupling (ECC) accounting for the directed motion of ligands through a membrane.[14−18] The corresponding rate constants depend on the conformations of a special membrane site (transporter) governed by a cyclically varied external electric field. As suggested previously,[19] an appropriately organized cyclic catalytic process of this kind can be regarded as a "catalytic wheel," pumping the particles from one reservoir to the other. The focus of the present work is on the development of the quantitative theory to describe the coupling of two processes, which underlies the mechanism of the catalytic wheel acting as a Brownian motor.

The kinetic scheme accounting for the occurrence of net circulations even in the absence of generalized external forces (such as concentration or potential gradients) is presented in section II. We consider a system consisting of two states, with the transitions between them occurring via two reaction channels. Rate constant modulations emerge as a result of the coupling between this system and a cyclic catalytic process. Two types of modulation are introduced: regular transitions occurring at definite instants and random Poisson flips between two regimes (labeled as "+" and "−"), each characterized by a fixed set of rate constant values. For regular switching, the net circulation flux in the stationary state can be represented as a sum of fluxes through a given channel averaged over the lifetimes of the + and − regimes. Thus, a branched chain of averaged fluxes through the effectively doubled number of states appears in the system under stationary conditions. In the case of random switching, we manipulate, from the outset, the probabilities of finding the system in one of four states (with the rate constant sets labeled by + and − for the corresponding regimes) and invoke average flux values. In both modulation

* Corresponding author. E-mail: vrozen@mail.kar.net.
† Institute of Atomic and Molecular Sciences, Academia Sinica.
‡ National Academy of Sciences of Ukraine.
§ Institute of Physics, Academia Sinica and University of Minnesota.

10.1021/jp048200a CCC: $27.50
Published on Web 09/15/2004

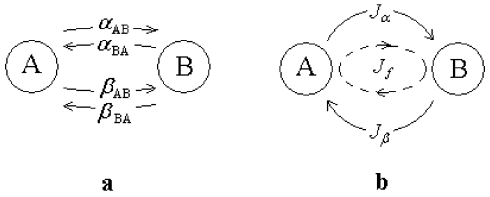

a **b**

Figure 1. Simple system with net circulation comprises two states, A and B, as well as two reaction channels, α and β, characterized by the rate constants (a) or by the corresponding fluxes (b).

cases, we arrive at the unified expression for the net circulation flux in which only one factor is sensitive to the switching type. As the analysis of this factor suggests, the net circulation flux is larger for regular than for random switching. Moreover, the net circulation flux is maximal at the equal relaxation-to-lifetime ratios for the + and − regimes. The significant inference is that the maximum efficiency of the input energy conversion to the mechanical energy of directed motion might be expected, provided an unbranched flux chain is in the system. This situation is referred to as the tight coupling limit, which occurs if the only reaction channel remains in either regime with the fixed set of rate constants.

In section III, the physical meaning of the parameters of the general scheme is elucidated by the concrete models, which also permits a further advance in the analytical treatment. An external cyclic process in the ECC model is represented by an external alternating electric field governing the ferment conformational states and hence the rate constants responsible for the transmembrane transfer of neutral ligands (subsection 1). In the flashing-potential model (for its antisymmetric variant, see ref 20), an external cyclic process controls the switching between the potential profiles and thus also causes the time dependence of the rate constants for surmounting potential barriers (subsection 2). As also shown (subsection 3), the parameters of the two models are interrelated, and the conclusions obtained for either model are valid for both. In the tight coupling limit (subsection 4), the optimal operational modes are realized when a motor works with the maximum output energy (useful work) or with the maximum efficiency, the latter reaching unity. The explanation of the high-efficiency mechanism is given by using the flashing potential model. The tight coupling limit is also considered in terms of the thermodynamics of irreversible processes, which enables generalized forces and the corresponding generalized fluxes to be introduced. The general conclusions of the study are given in section IV.

Two appendices to the paper contain detailed derivations of the expressions that clarify, from the general point of view, the origin of the net circulation flux and the tight coupling limit.

II. General Model

Consider a system that evolves by means of reaction transitions between states A and B. With a single reaction channel, the steady-state flux is always zero. Assume that the transitions can occur via two reaction channels α and β with rate constants $\alpha(\beta)_{AB}$ and $\alpha(\beta)_{BA}$ (Figure 1a). Let $P_{A(B)}$ be the probability of finding the system in a state A(B), $P_A + P_B = 1$. The time dependence $P_A(t)$ is governed by the equation

$$\frac{dP_A}{dt} = J_\beta - J_\alpha \tag{1}$$

where the fluxes through the α-channel J_α and the β-channel J_β are determined by

$$J_\alpha = \alpha_{AB}P_A - \alpha_{BA}P_B \qquad J_\beta = \beta_{BA}P_B - \beta_{AB}P_A \tag{2}$$

Directions of fluxes J_α and J_β are chosen so that the positive flux is clockwise (Figure 1b). In a steady state, when $dP_A/dt = 0$, the solution of eq 1 is given by

$$P_A = p_0 \equiv \frac{\xi_B}{\Sigma} \qquad \Sigma \equiv \xi_A + \xi_B \qquad \xi_A \equiv \alpha_{AB} + \beta_{AB} \qquad \xi_B \equiv \alpha_{BA} + \beta_{BA} \tag{3}$$

and the net circulation flux J is determined by flux $J_\alpha = J_\beta$:

$$J = \frac{\alpha_{AB}\beta_{BA} - \alpha_{BA}\beta_{AB}}{\Sigma} \equiv J_f \tag{4}$$

Thus, it is due to two reaction channels that the net circulation flux in a steady state becomes possible in principle. This possibility, however, can be realized only in a nonequilibrium steady state because an equilibrium implies the detailed balance condition

$$\alpha_{AB}\beta_{BA} - \alpha_{BA}\beta_{AB} = 0 \tag{5}$$

Interestingly, relationship 5 also holds true with time-dependent rate constants, which does not preclude the net circulation flux in a steady state.[21] A system with two reaction channels between two states can be regarded as the simplest model that permits the steady-state net circulation flux. It proves to be simpler than three-state and three-channel systems that are normally invoked as models for nonequilibrium steady-state circulation.[12,13,21−23] The treatment of the case with an arbitrary number of states/channels (using relationships similar to 1−5) is also available in the literature.[24]

The simplest trivial case when condition 5 is violated arises from the action on the system by a generalized external force f (a potential or concentration gradient), giving rise to the flux J_f (eq 4). A less trivial situation affording the generation of directed motion can occur in the absence of an external force, provided that the process concerned is coupled to another cyclic process, which results in time-dependent rate constants. If the cyclic process is a regular one and the rate constants are explicit functions of time, then eq 1 is solvable, and the corresponding solutions can be employed in the calculation of the time dependence of the flux. By averaging the flux over the period τ of the cyclic process for a sufficiently long time enabling the system to "forget" the initial conditions and go to the stationary state, we get the desired net circulation flux J. However, in the case of a random cyclic process, such a direct approach to the calculation fails. As an alternative, one can use the indirect approach, which involves, instead of the probability $P_{A(B)}$, the averaged probability $\rho_{A(B)} = \langle P_{A(B)} \rangle$, satisfying the master equation, with their contributions proportional to the mean cyclic frequencies of the process under consideration. The choice between the direct and indirect approaches resembles the situation emerging in the description of rate processes with dynamical disorder.[25] The two methods provide qualitatively similar results, and we arrive at unified relationships for the average net flux J in the stationary state. The two corresponding kinds of cyclic process are detailed further in this section.

First, we consider the case when the values of rate constant sets interchange with time regularly and periodically. Let the period τ comprise two time intervals, τ^+ and τ^- ($\tau = \tau^+ + \tau^-$), on which all rate constants have time-independent values. All of the quantities on the intervals $0 < t < \tau^+$ and $0 < t < \tau^-$ will be, respectively, labeled by the superscripts + and −.

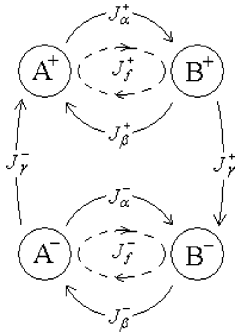

Figure 2. Diagram of the reaction channels arising from the switching between the + and − regimes.

The consideration of two rate constant regimes, + and −, is equivalent to going from the pair of states A and B to four states $A^{\pm}$ and $B^{\pm}$, with states A^+ and B^+ referring to time intervals τ^+ and A^- and B^- to τ^-. Instead of luxes J_α and J_β determined by eq 1, we now turn to fluxes $J_\alpha^\pm$ and $J_\beta^\pm$, which have been averaged over the period of the control cyclic process. The relevant computations (Appendix 1) suggest that unlike the no-switching case fluxes J_α^+ and J_β^+ become unequal, just as fluxes J_α^- and J_β^- do, whereas the differences $J_\gamma^\pm \equiv J_\alpha^+ - J_\beta^-$ and $J_\gamma^- \equiv J_\beta^- - J_\alpha^-$ are equal. Formally, the initiation of new fluxes $J_\gamma^\pm$ implies the emergence of new reaction channels between the states in two pairs: $B^+ \rightarrow B^-$ (flux J_γ^+) and $A^- \rightarrow A^+$ (flux J_γ^-). Figure 2 illustrates the change in the initial flux structure (Figure 1b) caused by the emergence of new reaction channels. This relation also suggests the important inference about the equality of the full net fluxes through channels α and β

$$J = \langle J_\alpha \rangle = \langle J_\beta \rangle \qquad \langle J_{\alpha,\beta} \rangle = J_{\alpha,\beta}^+ + J_{\alpha,\beta}^- \tag{6}$$

as it was in the no-switching case.

As opposed to the above treatment, where the flux picture shown in Figure 2 originated from the averaging over the periods of the control cyclic process, in the case of the random Poisson inter-regime switching, we a priori assume that Figure 2 refers to random transitions from states A^+ and B^+ to states A^- and B^- with rate constant γ^+ and to the reverse transitions with rate constant γ^-. Note that regular inter-regime switching implies that rate constants $\gamma^\pm$ are equal to the reciprocals of time intervals $\tau^\pm$. The frequencies of both regular and random inter-regime switching from + to − or from − to + are equal to the quantity $\gamma^+\gamma^-/\Gamma$, where $\Gamma = \gamma^+ + \gamma^-$. As shown in Appendix 1, fluxes $J_\alpha^\pm$, $J_\beta^\pm$, and J_γ in both regimes are determined by the equations

$$J_\alpha^\pm = \frac{\gamma^\mp}{\Gamma} J_f^\pm \pm \frac{\gamma^+\gamma^-}{\Gamma} \frac{\alpha_{AB}^\pm + \alpha_{BA}^\pm}{\Sigma^\pm}(p_0^- - p_0^+)\varphi$$

$$J_\beta^\pm = \frac{\gamma^\mp}{\Gamma} J_f^\pm \mp \frac{\gamma^+\gamma^-}{\Gamma} \frac{\beta_{AB}^\pm + \beta_{BA}^\pm}{\Sigma^\pm}(p_0^- - p_0^+)\varphi \tag{7}$$

$$J_\gamma = \frac{\gamma^+\gamma^-}{\Gamma}(p_0^- - p_0^+)\varphi \tag{8}$$

where $p_0^\pm$ and $J_f^\pm$ are given by eqs 3 and 4, respectively, and the explicit expressions for φ are different in the cases of regular and random switching as specified by eqs A1.8 and A1.12. We note that in the absence of a generalized external force all fluxes are proportional to the inter-regime switching frequencies, $\gamma^+\gamma^-/\Gamma$.

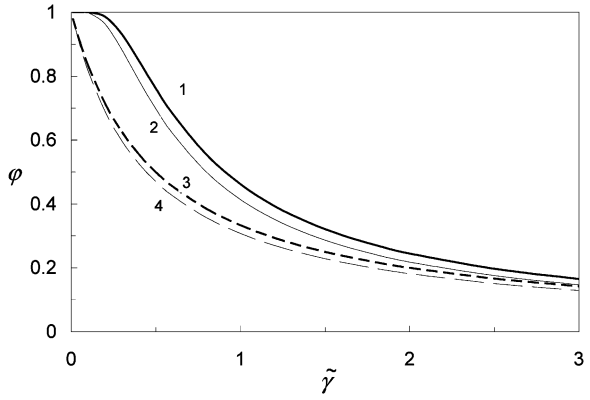

Figure 3. The dependence of the parameter φ on the reduced rate constant $\tilde{\gamma} = \tilde{\gamma}^+\tilde{\gamma}^-/2(\tilde{\gamma}^+ + \tilde{\gamma}^-)$ at $\tilde{\gamma}^+/\tilde{\gamma}^- = 1$ (bold lines 1 and 3) and $\tilde{\gamma}^+/\tilde{\gamma}^- = 2$ (thin lines 2 and 4) for the regular (solid lines 1 and 2) and random (dashed lines 3 and 4) switching.

We have thus developed a unified description for the origination of net circulation with the regular and random Poisson switching between the + and − regimes. The two switching modes differ only by the expressions for the quantity φ (symmetric functions of the parameters $\tilde{\gamma}^+$ and $\tilde{\gamma}^-$ in eqs A1.8 and A1.12). In both modes, the function φ tends to the same limits, 1 at $\tilde{\gamma}^\pm \rightarrow 0$ and $(\tilde{\gamma}^+ + \tilde{\gamma}^-)^{-1}$ at $\tilde{\gamma}^\pm \rightarrow \infty$. The parameters $\tilde{\gamma}^\pm$ characterize the ratios of the average relaxation times, $(\Sigma^\pm)^{-1}$, needed for the establishment of the stationary probability distributions in the + and − regimes to lifetimes $\tau^\pm$ of these regimes (or to their average lifetimes if random switching is concerned). The reciprocal values, $(\tilde{\gamma}^\pm)^{-1}$, specify the ratios of overall rate constants $\Sigma^\pm$ to switching rate constants $\gamma^\pm$. With the fixed sum $(\tilde{\gamma}^+)^{-1} + (\tilde{\gamma}^+)^{-1} \equiv 2/\tilde{\gamma}$, both functions reach their maxima at $\tilde{\gamma}^+ = \tilde{\gamma}^-$ (Figure 3). It is noteworthy that the function φ for the regular switching always exceeds its counterpart for the random switching as demonstrated by Figure 3. Because the φ-dependent contributions to the fluxes are proportional to φ, they will also have maximum values at the conditions indicated above.

Evidently, for the net circulation to occur, it is necessary that the energy be transferred to the system from the control cyclic process at the instants of +/− switching. The input energy imparted to the system in a unit time, W_{in}, is proportional to the probability flux, J_γ, arising from the inter-regime switching $+ \rightarrow - \rightarrow +$. Let U_{in} designate the corresponding proportionality coefficient. The useful work done against a generalized load force in a unit time, W_{out}, is proportional to the net circulation flux, J. With the corresponding proportionality coefficient denoted by U_{out}, the efficiency of the motor converting the input energy into the output energy of the directed motion can be written as

$$\eta \equiv \frac{W_{out}}{W_{in}} = \frac{U_{out}}{U_{in}} \frac{J}{J_\gamma} \tag{9}$$

We point out that there are a variety of alternative ways to define the input energy (and, hence, the efficiency) depending on the problem statement (see, e.g., refs 1, 9, and 26 and the literature therein). In what follows, we apply definition 9 because it has a natural relationship to the fluxes arising in the above kinetic description; thus, it is easy to introduce into the concrete models for which such a description holds.

Compare the magnitudes of fluxes J and J_γ. For definiteness, assume that $p_0^- - p_0^+ > 0$. The terms in eq 7 that are proportional to $\gamma^+\gamma^-/\Gamma$ will provide the contribution to J, which

is given by eq 8, accurate to the factor $[(\alpha^{+}_{AB} + \alpha^{+}_{BA})/\Sigma^{+} - (\alpha^{-}_{AB} + \alpha^{-}_{BA})/\Sigma^{-}]$. The latter expression (also assumed to be positive) is under unity by virtue of the inequalities $(\alpha^{\pm}_{AB} + \alpha^{\pm}_{BA})/\Sigma^{\pm} < 1$. The effect of the generalized load force leads to the violation of detailed balance condition 5 for the + and − regimes and hence to nonzero fluxes $J_f^{\pm}$ (eq 4). Because the load acts against the direction of the flux generated, $J_f^{\pm}$ should be negative. Thus, the inequality $J < J_\gamma$ should always hold true. The maximum efficiency is likely when the ratio J/J_γ tends to unity. As readily seen, one way to realize this condition is to leave a single reaction channel for either of the regimes, namely, channel α for the + regime and channel β for the − regime. Figure 2 exemplifies such a situation by one unbranched clockwise flux: $J^{+}_{\alpha} = J^{+}_{\gamma} = J^{-}_{\beta} = J^{-}_{\gamma}$. There are no reverse fluxes, J^{+}_{β} and J^{-}_{α}; as a result, fluxes $J_f^{\pm}$, accounting for the circulations within the + and − regimes, vanish as well. Note that the ratio J/J_γ can serve as a measure of the coupling between the external cyclic process and the one giving rise to the net circulation in the system concerned. At $J/J_\gamma \rightarrow 1$, the tight coupling limit is realized, with the coupling degree close to unity.[27,28]

To achieve the maximum possible efficiency $\eta \rightarrow 1$ with the proviso that $J \rightarrow J_\gamma$, the additional condition $U_{out} \rightarrow U_{in}$ must be met. However, the question of whether the two conditions are realizable together should be clarified in the framework of concrete models involving the detailed explicit expressions for rate constants α and β. Concrete models of this kind are addressed in the next section.

III. Particular Models

Here, we detail the general origin of the directed motion schematically represented in the previous section and exemplified by the model of electroconformational coupling (ECC) and the flashing-potential model. The two examples elucidate the physical meaning of the parameters of the general scheme and enable further advances in analytical calculations. Either model demonstrates how the catalytic wheel that results from the coupling of an external energy source to a motion-generating process can be organized with efficiency tending to unity. In the former model, two concrete coupling processes are discussed, the dependences of the main motor characteristics on the model parameters (see, e.g., ref 18) being not as transparent as those in the latter. The antisymmetric case of the flashing-potential model with randomly switching potentials was thoroughly considered in ref 20. The basic parameters of the ECC model are introduced in subsection 1. The general case of the flashing-potential model is analyzed in subsection 2. The relationship between the parameters of both approaches is established in subsection 3. Particular attention is given to the tight coupling limit; using it, we discuss the optimal basic characteristics of the motor that are valid for the most general problem statement (subsection 4).

1. Model of Electroconformational Coupling. The term electroconformational coupling (ECC) was introduced into molecular motor practice by Tsong and Astumian[14] to describe the conformational changes of a charged transporter that are induced by an external electric field and used to pump uncharged ligands across the membrane against a concentration gradient. A theory of this phenomenon was proposed later.[15−18] Each transporter can exist in the left or right conformation in which it can bind a ligand from the left or right bath (Figure 4). Because either transporter can contain a ligand or be free, four states result. Transitions between the left and right conformations

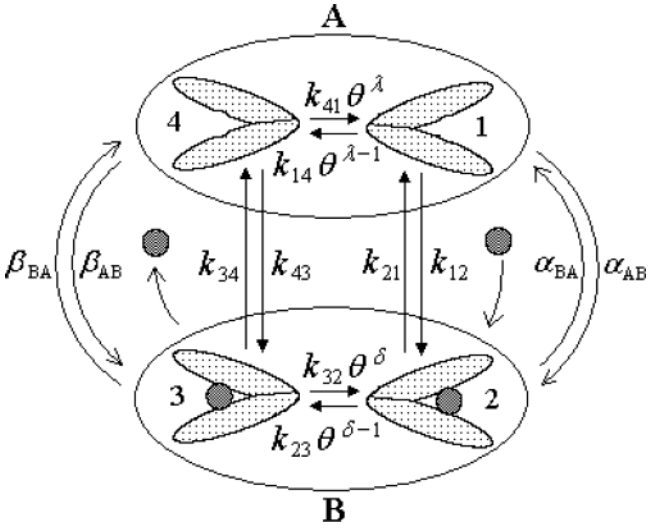

Figure 4. Basic parameters of the ECC model. States 1−4 correspond to the left and right transporter conformations with and without a ligand. The transitions between the states A and B representing the respective combinations of states 1,4 and 2,3 involve two reaction channels, α and β, through which the ligands get into the transporter from the right and left baths.

(1 ↔ 4 and 2 ↔ 3) can be governed by the potential of the applied electric field, Δ, which dictates the values of the corresponding rate constants (for designations see Figure 4) via the factor $\theta = \exp(ze\Delta/k_BT)$ (where z is the transporter valence, e is the elementary charge, k_B is the Boltzmann constant, and T is the absolute temperature).

The model reduces to that considered in section II, assuming that transitions 1 ↔ 4 and 2 ↔ 3 are extremely fast compared to other transitions.[15] Such an assumption allows for operating on the total probabilities P_A and P_B to find the system in states A and B, the two states representing the respective combinations of states 1, 4 and 2, 3. As a result, the probabilities of states 1−4 can be sought in the following form

$$P_1 = \kappa_A P_A \qquad P_4 = (1 - \kappa_A)P_A \qquad P_2 = \kappa_B P_B \qquad P_3 = (1 - \kappa_B)P_B \quad (10)$$

where

$$\kappa_A \equiv \frac{K_{14}\theta}{1 + K_{14}\theta} \qquad \kappa_B \equiv \frac{K_{23}\theta}{1 + K_{23}\theta} \qquad K_{14} = \frac{k_{41}}{k_{14}} \qquad K_{23} = \frac{k_{32}}{k_{23}} \quad (11)$$

Transitions between states A and B can involve either reaction channel α or β; these refer to the processes occurring to the right or to the left of the membrane, respectively

$$\alpha_{AB} = \kappa_A k_{12} \qquad \alpha_{BA} = \kappa_B k_{21} \qquad \beta_{AB} = (1 - \kappa_A)k_{43} \qquad \beta_{BA} = (1 - \kappa_B)k_{34} \quad (12)$$

Because transitions 1 → 2 and 4 → 3 imply the trapping of a ligand by the transporter from the right and left baths, with the ligand concentrations equal to C_r and C_l, respectively, the corresponding rate constants can be written as follows

$$k_{12} = \tilde{k}_{12}C_r \qquad k_{43} = \tilde{k}_{43}C_l \quad (13)$$

By substituting relationships 11−13 into 5, one can readily check that at equilibrium, when $C_l = C_r$, the detailed balance

condition takes the form

$$K_{14}\tilde{k}_{12}k_{34} = K_{23}k_{21}\tilde{k}_{43} \tag{14}$$

The particular case with $K_{14}K_{23} = 1$, $k_{12} = k_{34}$ and $k_{21} = k_{43}$ is referred to as the case of an antisymmetric transporter.[16]

The time dependence of the rate constants arises if the external electric field is time-dependent. The electric-field potential is considered to take on two values, $+\Delta$ and $-\Delta$ ($\Delta > 0$), with regular or random switching between the + and − regimes. The potential reversals will affect only the values of the parameter θ:$\theta^{\pm} \equiv \theta^{\pm 1}$; the rate constant values shown in 12, therefore, change upon going from one regime to the other (owing to the alternation of the parameters θ:$\kappa^{\pm}_{A(B)}$ specified by eq 11). It is along this pathway that the coupling between two processes results, and the catalytic wheel works in the ECC model. As a consequence, net circulation flux J is generated, which transports the ligands from the left to right bath (Figure 4) according to the formal flux diagram shown in Figure 2. The sought flux, J, defined by eq 6 can be calculated using relationships 7, A1.8, A1.12, and 12. Given J, it is a straightforward matter to find the useful work, W_{out}, done by the motor against the concentration gradient in a unit time in view of the fact that the work needed for a particle to be transferred from the left to the right bath equals $k_BT\ln(C_l/C_r)$. Thus, coefficient U_{out} measured in units of k_BT appears as

$$U_{out} = \ln\left(\frac{C_l}{C_r}\right) \tag{15}$$

Proportionality coefficient U_{in}, which relates the input energy imparted to the system in a unit time W_{in} to the probability flux J_γ is more complicated to determine. A direct way to calculate U_{in} as the rate of electric energy dissipation was proposed previously.[18] Here, we present another derivation of this quantity based on the juxtaposition of the ECC and flashing-potential models (subsection 3).

2. Flashing-Potential Model. Consider the hopping motion of a Brownian particle in a periodic asymmetric double-well potential $U(x)$ that describes the interaction between the particle and a track as a function of the particle position along the track. We also assume that the potential switching between the + and − regimes can take two forms, $U^+(x)$ and $U^-(x)$, but they are not identical and half-period-shifted as distinct from the antisymmetric case considered before.[20] The transitions between them may be caused by coupling with the control cyclic process, which may appear as an external signal or a far-from-equilibrium chemical reaction resulting in a conformational change of the particle or of the track. Either potential energy profile $U^{\pm}(x)$ is represented by a periodic sequence of wells A and B and barriers α and β labeled, respectively, by the superscript + or − (Figure 5) so that the transitions from potential well $A^+(B^+)$ of profile $U^+(x)$ are allowed only to potential well $A^-(B^-)$ of profile $U^-(x)$. The comparison of Figures 2 and 5 clearly shows that states $A^{\pm}(B^{\pm})$ and reaction channels $\alpha^{\pm}(\beta^{\pm})$ in the general model correspond to the potential wells and barriers in terms of the flashing-potential model. It is the periodic double-well potentials that give rise to the two reaction channels that are necessary for the net circulation flux to appear. Given the distribution of the well and barrier magnitudes shown in Figure 5, a particle initially found in well A^+ is expected to move into well B^+ to the right if the lifetime of regime + is large enough. After the potential has flipped to regime −, the particle presumably falls into well B^- from where it moves into well A^-, that is, to the right again. We can introduce potential energy Fx referring to load force $-F$ ($F > 0$) acting leftwards. Therefore, the coupling between the thermally activated surmounting of barriers and the potential modulation leads to the uphill flow of particles.

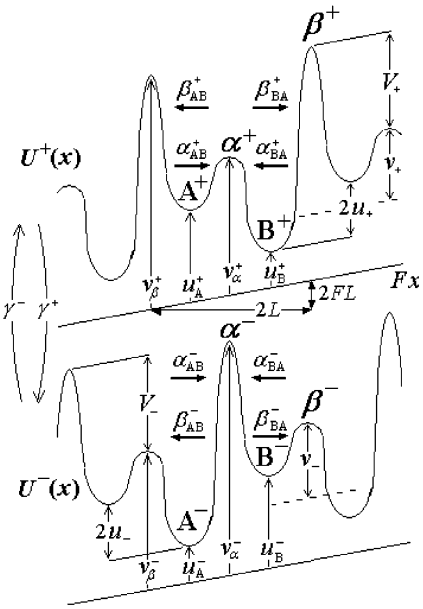

Figure 5. Two periodical potential profiles $U^{\pm}(x)$ of the flashing-potential model switching between the + and − regimes with the rate constants $\gamma^{\pm}$ in the external field of the load force $-F$ ($F > 0$). The depths of the wells $A^{\pm}(B^{\pm})$ and the heights of the barriers $\alpha^{\pm}(\beta^{\pm})$, along with the relevant profile characteristics and the rate constants referring to barrier surmounting, are indicated for both profiles.

The flashing-potential model has an additional advantage in the elucidation of the general scheme presented in section II: it enables us to illustrate the physical meaning of the rate constants well by expressing them in terms of the parameters of potentials $U^{\pm}(x)$ based on the Arrhenius-like expressions

$$\alpha^{\pm}_{AB} = k_0\exp(-v^{\pm}_\alpha + u^{\pm}_A - f) \qquad \alpha^{\pm}_{BA} = k_0\exp(-v^{\pm}_\alpha + u^{\pm}_B + f)$$

$$\beta^{\pm}_{BA} = k_0\exp(-v^{\pm}_\beta + u^{\pm}_B - f) \qquad \beta^{\pm}_{AB} = k_0\exp(-v^{\pm}_\beta + u^{\pm}_A + f) \tag{16}$$

(From here on all energy quantities are expressed in units of k_BT; $f = FL/(2k_BT)$; L is the half period of potentials $U^{\pm}(x)$; and k_0 is the intrawell relaxation frequency, which is the same for all wells). The values of the maxima $v^{\pm}_{\alpha(\beta)}$ and minima $u^{\pm}_{A(B)}$ for potential profiles $U^{\pm}(x)$ are indicated in Figure 5. Such a kinetic description is valid when the external modulation of the potential with rate constants $\gamma^{\pm}$ is slow compared to the parameter k_0 and when dimensionless barriers are greater than unity. When substituting eq 16 into 5, it is easy to verify that the detailed balance condition is met automatically at $f = 0$. The velocity of directed motion induced by the flips between the potential states is equal to the product of stationary flux J and period $2L$ of potentials $U^{\pm}(x)$. Because the useful work done against load force F in a unit time is equal to the product of the velocity and F, W_{out} is expressible as follows

$$W_{out} = U_{out}J \qquad U_{out} = 4f \tag{17}$$

As seen, proportionality coefficient U_{out} that relates W_{out} to J becomes quite comprehensible in terms of the flashing-potential model: U_{out} is merely the work done by load force F over a

period of $2L$ of the potentials $U^{\pm}(x)$. The coefficient of proportionality between the input energy per unit time, W_{in}, and the previously introduced (section II) flux, J_γ, is also easy to understand from the physical point of view. On each flip from potential well B^+ to B^- and from A^- to A^+, the particle gains the energy $u_B^- - u_B^+$ and $u_A^+ - u_A^-$, respectively. Multiplying these energies by corresponding fluxes $J_\gamma^{\pm}$, we arrive at

$$W_{in} = (u_B^- - u_B^+)J_\gamma^+ + (u_A^+ - u_A^-)J_\gamma^- = U_{in}J_\gamma \qquad (18)$$

where

$$U_{in} = 2(u_+ + u_-) \qquad u_+ \equiv \frac{(u_A^+ - u_B^+)}{2} \qquad u_- \equiv \frac{(u_B^- - u_A^-)}{2} \qquad (19)$$

(Equation 18 is derived with the equality $J_\gamma^+ = J_\gamma^-$, which was proven in section II.)

The potential well depths exhibited in Figure 5 are chosen to satisfy the conditions $u_A^+ > u_B^+$ and $u_B^- > u_A^-$; hence, $U_{in} > 0$. At $f = 0$, the quantities $p_0^{\pm}$ entering into eq 3 are determined by the relationship $p_0^{\pm} = [1 + \exp(u_A^{\pm} - u_B^{\pm})]^{-1}$, and the same conditions are therefore sufficient to provide the positive difference $p_0^- - p_0^+$ and, consequently, also positive fluxes J_γ and J. With increasing f, the wells on the right rise relative to the wells on the left, and negative fluxes $J_f^{\pm}$ grow at the same time. The two processes govern the behavior of the quantity $p_0^- - p_0^+$, which proves to vary with the parameter S, the summed differences of the relative barrier heights and well depths for potentials $U^{\pm}(x)$

$$S \equiv V_+ + V_- - 2(u_+ + u_-) \qquad (20)$$

where

$$V_+ \equiv v_\beta^+ - v_\alpha^+ \qquad V_- \equiv v_\alpha^- - v_\beta^- \qquad (21)$$

At $S < 0$, the inequality $p_0^- - p_0^+ > 0$ is valid for any value of f; that is, flux J_γ is always positive. At $S = 0$, the difference $p_0^- - p_0^+$ tends to go to zero if $f \to \infty$. Last, at $S > 0$, the equation $p_0^- - p_0^+ = 0$ has the root f_0 corresponding to the sign inversion point for flux J_γ. We note that f_0 is larger than $U_{in}/4$ and tends to $U_{in}/4$ at $S \gg 1$. Regarding flux J, it reaches, at a sufficiently large f, the stopping point ($f = f_s$) where its sign always reverses, irrespective of the S values (because of the growing negative fluxes $J_f^{\pm}$). The values of f_s always turn out to be smaller than $U_{in}/4$ and tend to $U_{in}/4$ at $S \gg 1$.

The inequality $S \gg 1$ implies that the barriers v_β^+ and v_α^- locking the backward motion are very high; that is, reaction channels β and α in regimes $+$ and $-$ are actually excluded from the branched flux chain in Figure 2, and fluxes J and J_γ level off. (See the end of section II.) At $f \to U_{in}/4$, the conditions $J \to J_\gamma$ and $U_{out} \to U_{in}$ are fulfilled together so that the efficiency tends to unity according to eq 9. This limiting effect of importance is given much attention in subsection 4.

3. Comparison of Two Models. A qualitative analogy between the ECC model and the Brownian motion of a particle in a periodic potential was pointed out in the literature.[19,29−31] We find it very instructive to correlate the parameters and main characteristics of the two models quantitatively. As external parameters, the ECC and flashing-potential models involve concentration and load force, respectively, which are related via expressions 15 and 17 for U_{out}

$$\frac{C_l}{C_r} = \exp(4f) \qquad (22)$$

The relationship between the internal parameters of the models concerned is established by equating the corresponding rate constants 12 (with regard to eq 11) and 16 at $C_l = C_r$ and $f = 0$

$$\theta^2 = \exp(V_+ + V_-) \qquad (23)$$

$$\frac{(1 + K_{23}\theta)(\theta + K_{14})}{(1 + K_{14}\theta)(\theta + K_{23})} = \exp(U_{in}) \qquad (24)$$

(For an explicit expression of U_{in} in terms of the parameters of the flashing-potential model, see eq 19.) Potential barriers fulfill the same role in the flashing-potential model as parameter θ in the ECC model. Accordingly, the potential well depths are related to parameters K_{14} and K_{23}. The antisymmetric flashing-potential model discussed previously[20] corresponds to a particular case of the antisymmetric transporter, as both models imply $\alpha_{AB}^{\pm} = \beta_{BA}^{\mp}$ and $\alpha_{BA}^{\pm} = \beta_{AB}^{\mp}$. Note that the expression for W_{in} obtained in view of eqs 8 and 24 coincides with that derived in ref 18 by another method.

Owing to relations 22−24, the conclusions made for either model prove to be valid for both. For example, the statement[18] that the quantity W_{in} can be invariably positive or change sign with increasing concentration ratio C_l/C_r, as dictated by the values of parameter θ, follows from the analysis of the behavior of the difference $p_0^- - p_0^+$ in relation to parameter S specified by eq 20. As another example, the large values of electric-pulse potentials ($\theta \gg 1$) correspond to the large values of parameter S, that is, to the extremely different heights for the barriers locking the backward fluxes in each potential. It is in this limit that the highest possible efficiency of the motor is achieved, and this limiting case is investigated more closely in the next subsection.

4. Tight Coupling Limit. The ECC and flashing-potential models are both characterized by a large number of parameters governing the main operational characteristics of the motor, viz., J, W_{out}, and η. In previous studies, J and η were plotted versus the concentration ratio C_l/C_r with certain parameter sets typical of the antisymmetric transporter at regularly switched electric pulses[18] and also versus load force f in terms of the antisymmetric flashing-potential model with randomly switched half-period-shifted potentials.[20] Also, consideration was given to the asymptotic behavior of the efficiency η at high barriers locking the backward motion of a Brownian particle.[20] At the same time, the limit of high barriers ($V_{\pm} \to \infty$, with $V_{\pm}$ defined by eq 21) makes it possible to obtain a manifold of analytical dependences for the quantities of interest (Apendix 2). This limit referred to as the tight coupling limit enables us to conveniently study the extremal behavior not only for the efficiency η at arbitrary parameters of potentials $U^{\pm}(x)$ switched regularly or randomly but also for another significant motor characteristic, W_{out}, accounting for the ability to do useful work against the load force. Just the maximum value of W_{out} reached at large, though not maximum, values of η is the most relevant to the motor operational mode. Appendix 2 demonstrates that the behavior of the function $W_{out}(f)$ varies according to the differences in the well depths $u^{\pm}$ and the relative modulation rate constants $\tilde{\gamma}^{\pm}$. Provided the efficiency is high ($\eta \geq 0.5$), the maximum of W_{out} can be reached at $u_{\pm} \ll 1$ and arbitrary $\tilde{\gamma}^{\pm}$ or at $u^{\pm} > 1$ and $\tilde{\gamma}^{\pm} \ll 1$. The value W_{out} is, however, small in both cases because of the smallness of the parameters $u_{\pm}$ or $\tilde{\gamma}^{\pm}$. As with

usual motors, large values W_{out} are reached at relatively low efficiencies η.

The consideration of the tight coupling limit leads to the conclusion of most significance: at $V_{\pm} \gg 1$, the maximum efficiency is reached at $f \approx U_{in}/4$ and tends to unity by the following law

$$\eta_m \approx 1 - 2\sqrt{(\zeta^+\epsilon^+ + \zeta^-\epsilon^-)\varphi^{-1}} \qquad (25)$$

Here, the $\zeta^{\pm}$ values are proportional to the average number of surmountings of low barriers, which occur in the average lifetime of the + or − regime, $\epsilon^{\pm}$ designates the small parameters proportional to $\exp(-V^{\pm})$, and φ is specified by eq A1.8 or A1.12. As noted in section II, net flux J has the maximum values, provided there is regular switching of the potentials with $\tilde{\gamma}^+ = \tilde{\gamma}^-$. A similar inference follows from eq 25 for the efficiency η_m: it reaches a maximum at the maximum values of φ with $\zeta^+ = \zeta^-$. In the case of $\gamma^+ = \gamma^-$, the condition $\zeta^+ = \zeta^-$ is met for the antisymmetric models with $\alpha^{\pm}_{AB} = \beta^{\mp}_{BA}$ and $\alpha^{\pm}_{BA} = \beta^{\mp}_{AB}$. Thus, the antisymmetric models of ECC and the flashing-potential represent more than mere simplifications conveniently reducing the number of parameters in the description; they also provide the best possible values of the main motor characteristics.

The particular models considered provide insight into the intimate physical meaning of eq 9 specifying motor efficiency. The quantity U_{in} appears as a driving force, giving rise to net circulation flux J. The characteristics U_{in} and U_{out} can be regarded as generalized forces. In the linear approximation of these quantities, they correspond to fluxes J_γ and J, which are equal to the partial derivatives of entropy production with respect to these generalized forces. As shown in ref 27, a measure of the degree of coupling, q, is expressible in terms of a certain combination of the Onsager coefficients entering into the expansion J_γ and J in U_{in} and U_{out}. With relationships 6−8 and 16−21, the Onsager coefficients are easily calculable, and it becomes evident that the tight coupling limit ($q \to 1$) is reached just at $S \gg 1$ ($V_{\pm} \to \infty$). In this case, we arrive at $\eta_m \approx 1 - 2\sqrt{1-q^2}$, where $q \approx 1 - (\zeta^+\epsilon^+ + \zeta^-\epsilon^-)\varphi^{-1}/2$ and $\epsilon^{\pm} \approx 2\exp(-V_{\pm})$. An important inference that is apparent from eq 25 is that the quantities U_{in} and U_{out} need not be small for the tight coupling limit to be reached.

Nonzero values of the driving force U_{in} arise from the asymmetry of potentials $U^{\pm}(x)$, which represents a necessary condition for the net circulation flux occurrence and can be introduced variously. For instance, the model suggested in ref 32 implies that the symmetry is broken by the dynamics of potential fluctuations rather than by using a spatial asymmetric potential. It is noteworthy that in terms of the flashing-potential model high motor efficiency results not only from the high barriers $V_{\pm} \to \infty$ but also from the relative shift by half a period, L, of potential wells A and B, which allows for transitions only between the minima of these potential wells. The Fokker−Planck description of the flashing-potential model with an arbitrary potential relief demonstrates the significance of an additional condition, viz., identically shaped and energy-shifted (by $2u_{\pm}$ as in Figure 5) potential portions on half periods L.[33]

IV. Conclusions

We have considered, from the general point of view, the origin of the net circulation flux in a system involved in a so-called catalytic wheel: transitions between states A and B of the system occur via two reaction channels, with their characteristics (transition rate constants) governed by an external cyclic process that "catalyzes" the directed motion generation. A uniform description is provided for regular and random switching between the + and − regimes, each characterized by a certain rate constant set. The basic operational characteristics of the Brownian motor in the stationary state prove to be optimal, provided there is regular switching as well as equal relaxation-to-lifetime ratios for + and − regimes. Under stationary conditions, there arises a branched chain of average fluxes through the doubled number of states $A^{\pm}$ and $B^{\pm}$. The maximum efficiency of the input energy conversion to the mechanical energy of directed motion is reached just for the unbranched flux chain, that is, in the tight coupling limit. This situation results from locking the backward flux or, in other words, ruling out the second reaction channel in each regime.

As a particular realization of the general scheme, the ECC model and the flashing-potential model are considered. The former exploits, as an external cyclic process, an external alternating electric field governing the ferment conformational states and, hence, the rate constants responsible for the transmembrane transfer of neutral ligands. The tight coupling limit is reached by the enhanced amplitudes of the electric-field pulses. In the latter model, an external cyclic process controls the switching between the potential profiles and thus gives rise to the time-dependent rate constants for surmounting the potential barrier. At sufficiently large differences in the potential barrier heights, backward fluxes prove to be locked; that is, the tight coupling limit is realized. The flashing-potential model demonstrates well that the catalytic wheel under consideration functions as a Brownian motor. From the comparison of the two models, it follows that their parameters are interrelated, and a conclusion obtained for any of them can be extended to the other. In the case of equal lifetimes (switching rate constants), the optimal operational characteristics are afforded by the "antisymmetric transporter" of the ECC model, which corresponds to switching between half-period-shifted potentials in terms of the flashing-ratchet model. Thus, the antisymmetric models are not only useful simplifications reducing the number of parameters but also provide the best possible values for the main motor characteristics, such as the net circulation flux, the output energy (useful work), and the efficiency.

In the limit of tight coupling, simple analytical expressions are derived that relate the basic operational characteristics of the motor to the load force. The optimal working modes provided by tight coupling are also analyzed, and the necessary conditions are formulated for both the maximum output energy and the maximum efficiency of the motor. As shown, the maximum efficiency in this limit can reach unity.

Acknowledgment. We thank Dr. M. L. Dekhtyar for her helpful comments on the manuscript. This work was supported by Academia Sinica. V.M.R. gratefully acknowledges the kind hospitality received from the Institute of Atomic and Molecular Sciences.

Appendix 1. Deduction of Equations for Regular and Random Inter-Regime Switching

For regular inter-regime switching, let the current time be characterized by the set of three variables, $\{n, \pm, t\}$, two of them discrete and one continuous, so that $n = 0, 1, 2, \ldots$ enumerates the periods of the cyclic process and the index + or − refers to the respective time interval τ^+ or τ^- within which the continuous time variable t is defined. With this notation, the general solution of the differential eq 1 valid for either time

interval appears as

$$P^{\pm}_{A,(n)}(t) = p_0^{\pm} + C^{\pm}_{A,(n)} \exp(-\Sigma^{\pm} t) \qquad \text{(A1.1)}$$

Here, $p_0^{\pm}$ is given by eq 3, and arbitrary constants $C^{\pm}_{A,(n)}$ are specified by the boundary conditions

$$P^{-}_{A,(n-1)}(\tau^{-}) = P^{+}_{A,(n)}(0) \qquad P^{+}_{A,(n)}(\tau^{+}) = P^{-}_{A,(n)}(0) \quad \text{(A1.2)}$$

On substituting eq A1.1 into A1.2, the recurrent relationships for $C^{\pm}_{A,(n)}$ are easily obtained

$$C^{+}_{A,(n)} = C^{-}_{A,(n-1)} E^{-} - (p_0^{+} - p_0^{-}) \qquad E^{\pm} \equiv \exp(-\Sigma^{\pm}\tau^{\pm})$$

$$C^{-}_{A,(n)} = (1 - E^{+})(p_0^{+} - p_0^{-}) + E^{+}E^{-} C^{-}_{A,(n-1)} \qquad \text{(A1.3)}$$

The latter expression is used to express $C^{-}_{A,(n)}$ in terms of the initial value $C^{-}_{A,(0)}$ (invoking the summation of the geometric progression)

$$C^{-}_{A,(n)} = \frac{(1 - E^{+})(p_0^{+} - p_0^{-})}{1 - E^{+}E^{-}}[1 - (E^{+}E^{-})^{n}] + (E^{+}E^{-})^{n} C^{-}_{A,(0)} \qquad \text{(A1.4)}$$

Note that $E^{+}E^{-} < 1$. The stationary state, therefore, corresponds to those periods n of the cyclic process that admit neglecting the factors $(E^{+}E^{-})^{n}$, hence implying that the system "forgets" the initial value $C^{-}_{A,(0)}$. Thus, probabilities $P^{\pm}_{A}(t)$ in the stationary state will depend only on the current instant of time t within either time interval + or −

$$P^{\pm}_{A}(t) = p_0^{\pm} \mp \frac{(1 - E^{\mp})(p_0^{-} - p_0^{+})}{1 - E^{+}E^{-}} \exp(-\Sigma^{\pm} t) \quad \text{(A1.5)}$$

(A similar solution for the particular case $\tau^{+} = \tau^{-}$ was derived previously.[18])

Fluxes J_α and J_β are determined by eq 1 as before, but they are now functions of time because of the time dependence of probability $P^{\pm}_{A}(t)$. Our concern is with the fluxes averaged over the period of the control cyclic process

$$\langle J_{\alpha,\beta} \rangle \equiv \frac{1}{\tau}\{\int_0^{\tau^{+}} J^{+}_{\alpha,\beta}(t)\mathrm{d}t + \int_0^{\tau^{-}} J^{-}_{\alpha,\beta}(t)\mathrm{d}t\} = J^{+}_{\alpha,\beta} + J^{-}_{\alpha,\beta}$$

$$J^{\pm}_{\alpha} \equiv \alpha^{\pm}_{AB}\,\rho^{\pm}_{A} - \alpha^{\pm}_{BA}\,\rho^{\pm}_{B} \qquad J^{\pm}_{\beta} \equiv \beta^{\pm}_{BA}\,\rho^{\pm}_{B} - \beta^{\pm}_{AB}\,\rho^{\pm}_{A} \qquad \text{(A1.6)}$$

The quantities $\rho^{\pm}_{A(B)}$ introduced here are the average probabilities of finding the system in a state A(B) on the time intervals + and −

$$\rho^{\pm}_{A} \equiv \frac{\tau^{\pm}}{\tau}\bar{P}^{\pm}_{A} \qquad \rho^{\pm}_{B} \equiv \frac{\tau^{\pm}}{\tau}(1 - \bar{P}^{\pm}_{A})$$

$$\bar{P}^{\pm}_{A} \equiv \frac{1}{\tau^{\pm}}\int_0^{\tau^{\pm}} P^{\pm}_{A}(t)\,\mathrm{d}t = p_0^{\pm} \pm \tilde{\gamma}^{\pm}(p_0^{-} - p_0^{+})\varphi \quad \text{(A1.7)}$$

where

$$\varphi \equiv \frac{(1 - E^{+})(1 - E^{-})}{1 - E^{+}E^{-}} = \frac{2\sinh\left(\frac{1}{2\tilde{\gamma}^{+}}\right)\sinh\left(\frac{1}{2\tilde{\gamma}^{-}}\right)}{\sinh\left(\frac{1}{2\tilde{\gamma}^{+}} + \frac{1}{2\tilde{\gamma}^{-}}\right)}$$

$$\tilde{\gamma}^{\pm} \equiv \frac{\gamma^{\pm}}{\Sigma^{+}} \qquad \gamma^{\pm} \equiv (\tau^{\pm})^{-1} \qquad \text{(A1.8)}$$

By substituting eq A1.7 into A1.6 with regard for the identity $\tau^{\pm}/\tau = \gamma^{\mp}/\Gamma$ (where $\Gamma = \gamma^{+} + \gamma^{-}$), we obtain eq 7. It is straightforward to show that for flux differences $J^{\pm}_{\alpha}$ and $J^{\pm}_{\beta}$ the following equalities hold: $J_\gamma \equiv J^{+}_{\gamma} = J^{-}_{\gamma}$, with the quantity J_γ specified by eq 8. It is noteworthy that fluxes $J^{\pm}_{\gamma}$ can be found directly from Figure 2, with an allowance made for the fact that rate constants α and β undergo a jumplike change at instants τ^{+} and τ^{-}

$$J^{+}_{\gamma} = \gamma^{+} P^{+}_{B}(\tau^{+}) - \gamma^{-} P^{-}_{B}(\tau^{-})$$

$$J^{-}_{\gamma} = \gamma^{-} P^{-}_{A}(\tau^{-}) - \gamma^{+} P^{+}_{A}(\tau^{+}) \quad \text{(A1.9)}$$

On substituting expressions A1.5 into this relation, it turns out that both fluxes are represented by eq 8.

In the case of random Poisson inter-regime switching, the master equation for probabilities $\rho^{\pm}_{A(B)}$ to find the system in states $A^{\pm}(B^{\pm})$ becomes

$$\frac{\mathrm{d}}{\mathrm{d}t}\begin{pmatrix}\rho^{+}_{A}\\ \rho^{+}_{B}\\ \rho^{-}_{A}\\ \rho^{-}_{B}\end{pmatrix} = \begin{pmatrix}-\xi^{+}_{A} - \gamma^{+} & \xi^{+}_{B} & \gamma^{-} & 0\\ \xi^{+}_{A} & -\xi^{+}_{B} - \gamma^{+} & 0 & \gamma^{-}\\ \gamma^{+} & 0 & -\xi^{-}_{A} - \gamma^{-} & \xi^{-}_{B}\\ 0 & \gamma^{+} & \xi^{-}_{A} & -\xi^{-}_{B} - \gamma^{-}\end{pmatrix}\begin{pmatrix}\rho^{+}_{A}\\ \rho^{+}_{B}\\ \rho^{-}_{A}\\ \rho^{-}_{B}\end{pmatrix} \qquad \text{(A1.10)}$$

The stationary solution of eq A1.10 can be written in a form similar to eq A1.7

$$\rho^{\pm}_{A} = \frac{\gamma^{\mp}}{\Gamma}\bar{P}^{\pm}_{A} \qquad \rho^{\pm}_{B} = \frac{\gamma^{\mp}}{\Gamma}(1 - \bar{P}^{\pm}_{A})$$

$$\bar{P}^{\pm}_{A} \equiv p_0^{\pm} \pm \tilde{\gamma}^{\pm}(p_0^{-} - p_0^{+})\varphi \quad \text{(A1.11)}$$

with the function φ of the parameters $\tilde{\gamma}^{\pm}$ appearing as

$$\varphi = (1 + \tilde{\gamma} + \tilde{\gamma}^{-})^{-1} \qquad \text{(A1.12)}$$

(cf. with eq A1.8). Explicit expressions 6 and 7 for net flux J as well as relationship 8 for J_γ retain their form, taking into account eq A1.12 for the function φ. Equations A1.9, however, change to the relations

$$J^{+}_{\gamma} = \gamma^{+}\rho^{+}_{B} - \gamma^{-}\rho^{-}_{B} \qquad J^{-}_{\gamma} = \gamma^{-}\rho^{-}_{A} - \gamma^{+}\rho^{+}_{A} \qquad \text{(A1.13)}$$

which follow directly from master eq A1.10. By substituting eq A1.11 into A1.13, it is easy to verify that both fluxes are given by eq 8. In terms of the antisymmetric model, with $\alpha^{\pm}_{AB} = \beta^{\mp}_{BA}$, $\alpha^{\pm}_{BA} = \beta^{\mp}_{AB}$, the relations derived for probabilities $\rho^{\pm}_{A(B)}$ and net flux J reduce to those obtained previously.[20]

Appendix 2. Analytical Dependences for the Tight Coupling Limit

In consideration of the limit $V_{\pm} \to \infty$, it is reasonable to study two variation ranges for load force f, namely, out of and within the vicinity of the point $U_{in}/4$. Proceeding to the limit $V_{\pm} \to \infty$

in the former region leads to

$$J = J_\gamma = \frac{\gamma^+\gamma^-}{2\Gamma}\varphi[\tanh(u_+ - f) + \tanh(u_- - f)]$$

$$W_{out} = 4fJ \qquad \eta = \frac{2f}{u_+ + u_-} \quad \text{(A2.1)}$$

($u^\pm$ is given by eq 19). Equation A2.1 formally suggests that the fluxes vanish at $f = (u_+ + u_-)/2 = U_{in}/4$. As a result, the differences between barriers $V_\pm$ cannot be regarded as infinite in the latter region ($f \to U_{in}/4$) because small quantities of the order $f - U_{in}/4$ compete with small $V_\pm$-dependent parameters discussed at the end of this Appendix.

Let us analyze the f dependence of W_{out} in the first variation range of f. It should be borne in mind that the function φ can also depend on f via the quantity $\Sigma^\pm$ (see eqs 3, A1.8, A1.12, and 19), which assumes the following form in the limit $V_\pm \to \infty$

$$\Sigma^\pm = 2k_0 \exp(-v_\pm)\cosh(u_\pm - f) \quad \text{(A2.2)}$$

Here, parameters $v_\pm$ specify the heights of low barriers relative to the average depths of potential wells

$$v_+ \equiv v_\alpha^+ - \frac{(u_A^+ + u_B^+)}{2} \qquad v_- \equiv v_\beta^- - \frac{(u_A^- + u_B^-)}{2} \quad \text{(A2.3)}$$

If the well depths differ slightly ($f < u_\pm \ll 1$), then the f dependence of $\Sigma^\pm$ can be neglected and the quantity W_{out} is proportional to the factor $f(u_+ + u_- - 2f)$, reaching its maximum at $f = (u_+ + u_-)/4$. This point corresponds to $\eta = 0.5$. At strongly different well depths ($u_\pm > 1$), the f dependences of $\Sigma^\pm$ and φ are significant, which leads to the radically different behavior of W_{out} at low ($\tilde\gamma^\pm \ll 1$) and high ($\tilde\gamma^\pm \gg 1$) relative modulation rate constants. To illustrate this inference, we restrict ourselves to the antisymmetric model, which operates on $v_+ = v_- \equiv v$ and $u_+ = u_- \equiv u$.

Because $\varphi \to 1$ at $\tilde\gamma \ll 1$, W_{out} is proportional to $f\tanh(u - f)$. This function has a maximum if $2f = \sinh 2(u - f)$; at $u \gg 1$, this condition provides $f \approx u - (\ln 4u)/2$ and $\eta \approx 1 - (\ln 4u)/2u$. In the inverse limit $\tilde\gamma \gg 1$, we have $\varphi \to (2\tilde\gamma)^{-1}$. Then W_{out} is proportional to $f\sinh(u - f)$, with its maximum reached on the condition that $f = \tanh(u - f)$. Hence, at $u \gg 1$ we obtain $f \approx 1$ and $\eta \approx {}^1/_u$.

We now turn to the analysis of the extremal properties of efficiency η in the second variation range of f, where $f \to (u_+ + u_-)/2$. The quantities $V_\pm$ will be considered in the linear approximation with respect to the small parameters

$$\epsilon^\pm \equiv \frac{2}{u_+ + u_-}\sinh(u_+ + u_-)\exp(-V_\pm) \quad \text{(A2.4)}$$

Fluxes J and J_γ are no longer equal and vanish at the respective values $f = f_s$ and $f = f_0$, differing by the value of the order $\epsilon^\pm$

$$J \approx \Lambda(f_s - f) \qquad J_\gamma \approx \Lambda(f_0 - f)$$

$$\Lambda \equiv \frac{\gamma^+\gamma^-}{\Gamma}\varphi\cosh^{-2}\left(\frac{u_+ - u_-}{2}\right) \quad \text{(A2.5)}$$

$$f_s \approx \frac{u_+ + u_-}{2}(1 - \delta_s) \qquad f_0 \approx \frac{u_+ + u_-}{2}(1 + \delta_0) \quad \text{(A2.6)}$$

$$\delta_s = \varphi^{-1}(\zeta^+\epsilon^+ + \zeta^-\epsilon^-) - \delta_0 \qquad \delta_0 = \frac{1}{2}(\epsilon^+ + \epsilon^-) \quad \text{(A2.7)}$$

Here, $\zeta^\pm \equiv (2\tilde\gamma^\pm)^{-1} = \Sigma^\pm/2\gamma^\pm$ and $\Sigma^\pm$ is given by A2.2 with $f = (u_+ + u_-)/2$ so that we arrive at

$$\zeta^\pm = \frac{k_0\exp(-v_\pm)}{\gamma^\pm}\cosh\left(\frac{u_+ - u_-}{2}\right) \quad \text{(A2.8)}$$

In the case of $u_+ = u_-$, the quantities $\zeta^\pm$ have a clear physical meaning: they determine the average number of surmountings of low barriers, which occur in the average lifetime of the + or − regime.

With relationships A2.5 and A2.6, expression 9 for the efficiency can be rewritten as

$$\eta \approx \frac{2f}{u_+ + u_-}\frac{f_s - f}{f_0 - f} = \frac{(z - \delta_s)(1 - z)}{z + \delta_0} \qquad z \equiv 1 - \frac{2f}{u_+ + u_-} \quad \text{(A2.9)}$$

The function $\eta(z)$ has its maximum η_m at the point $z = z_m$

$$\eta_m = 1 - 2z_m + \delta_s \qquad z_m = \sqrt{(\delta_0 + \delta_s)(1 + \delta_0)} - \delta_0 \quad \text{(A2.10)}$$

Because δ_0 and δ_s are proportional to the small parameters $\epsilon^\pm$, η_m tends to unity at $\epsilon^\pm \to 0$ by the square root law. The characteristic values of the load force obey the inequalities $f_m < f_s < (u_+ + u_-)/2 < f_0$, with the difference between f_s and f_0 comprised by terms of the order $\epsilon^\pm$ and between f_m and f_s by terms of the order $\sqrt{\epsilon^\pm}$.

Note Added in Proof. After our manuscript was accepted for publication, we were informed by Dr. Dean Astumian and Dr. Hong Qian about a paper by J. Wyman, which treated enzyme steady states as the "turning wheel". (Wyman, J. *Proc. Natl. Acad. Sci. U.S.A.* **1975**, *72*, 3983−3987.) The term "catalytic wheel" was first used in relation to this work. (Tsong, T. Y. *Adv. Chem. Ser.* **1995**, *235*, 561−578.) The former work deals with coupled chemical reactions, and the latter deals with conformational oscillations and fluctuations as the core mechanisms for energy coupling. Further study is underway.

References and Notes

(1) Reimann, P. *Phys. Rep.* **2002**, *361*, 57.
(2) Astumian, R. D. *Science* **1997**, *276*, 917.
(3) Jülicher, F.; Ajdari, A.; Prost, J. *Rev. Mod. Phys.* **1997**, *69*, 1269.
(4) *Appl. Phys. A* **2002**, *75*, 167−352, special issue on ratchets and Brownian motors: basic experiments and applications, edited by H. Linke.
(5) Porto M.; Urbakh, M.; Klafter, J. *Phys. Rev. Lett.* **2000**, *84*, 6058.
(6) Popov V. L. *Phys. Rev. E* **2003**, *68*, 026608.
(7) Rousselet, J.; Salome, L.; Adjari, A.; Prost, J. *Nature.* **1994**, *370*, 446. Faucheux, L. P.; Bourdieu, L. S.; Kaplan, P. D.; Libchaber, A. J. *Phys. Rev. Lett.* **1995**, *74*, 1504.
(8) Mitsui, T.; Oshima, H.; *J. Musc. Res. Cell Motil.* **1988**, *9*, 248.
(9) Magnasco, M. O. *Phys. Rev. Lett.* **1994**, *72*, 2656.
(10) Astumian, R. D.; Bier, M. *Biophys. J.* **1996**, *70*, 637.
(11) Keller, D.; Bustamante, C. *Biophys. J.* **2000**, *78*, 541.
(12) Qian, H.; Qian, M. *Phys. Rev. Lett.* **2000**, *84*, 2271.
(13) Qian, H.; Elson, E. L. *Biophys. Chem.* **2002**, *101*, 565.
(14) Tsong, T. Y.; Astumian, R. D. *Bioelectrochem. Bioenerg.* **1986**, *15*, 457.
(15) Markin, V. S.; Tsong, T. Y.; Astumian, R. D.; Robertson, R. *J. Chem. Phys.* **1990**, *93*, 5062.
(16) Markin, V. S.; Tsong, T. Y. *Biophys. J.* **1991**, *59*, 1308.
(17) Markin, V. S.; Tsong, T. Y. *Bioelectrochem. Bioenerg.* **1991**, *26*, 251.
(18) Chen, Y.; Tsong, T. Y. *Biophys. J.* **1994**, *66*, 2151.
(19) Tsong T. Y.; Chang, C.-H. *AAPPS Bulletin* **2003**, *13*, 12.
(20) Makhnovskii, Yu. A.; Rozenbaum, V. M.; Yang, D.-Y.; Lin, S. H.; Tsong, T. Y. *Phys. Rev. E* **2004**, *69*, 021102.
(21) Astumian, R. D. *Appl. Phys. A* **2002**, *75*, 193.
(22) Qian, H. *Biophys. Chem.* **1997**, *67*, 263.
(23) Qian, H. *Phys. Rev. E* **2001**, *64*, 022101.
(24) Tomita, K.; Tomita, H. *Prog. Theor. Phys.* **1974**, *51*, 1731.

(25) Zwanzig, R. *Acc. Chem. Res.* **1990**, *23*, 148.
(26) Parmeggiani A.; Jülicher, F.; Ajdari, A.; Prost, J.*Phys. Rev. E* **1999**, *60*, 2127.
(27) Kedem O.; Caplan S. R. *Trans. Faraday Soc.* **1965**, *61*, 1897.
(28) Caplan S. R.; Essig, A. *Bioenergetics and Linear Nonequilibrium Thermodynamics*; Harvard University Press: Cambridge, MA, 1983; chapter 4.
(29) Astumian, R. D. *J. Phys. Chem.* **1996**, *100*, 19075.
(30) Tsong, T. Y.; Xie, T. D. *Appl. Phys. A* **2002**, *75*, 345
(31) Tsong T. Y.; Chang, C.-H. *Physica A* **2003**, *321*, 124.
(32) Fleishman, D.; Filippov, A. E.; Urbakh M. *Phys. Rev. E* **2004**, *69*, 011908.
(33) Rozenbaum, V. M. *Pis'ma Zh. Eksp. Teor. Fiz.* **2004**, *79*, 475 (*JETP Lett.* **2004**, *79*, 388).